PHYSICAL REVIEW C VOLUME 9, NUMBER 6 JUNE 1974

Quasielastic electron scattering

R. R. Whitney* and I. Sick†
High Energy Physics Laboratory and Department of Physics, Stanford University,‡ Stanford, California 94305

and

J. R. Ficenec, R. D. Kephart,§ and W. P. Trower
Physics Department, Virginia Polytechnic Institute and State University,¶ Blacksburg, Virginia 24061

(Received 31 January 1974)

Data and interpretation are presented for inelastic electron scattering in the quasielastic region from nine target nuclei ranging from lithium to lead at an incident energy of 500 MeV and a scattering angle of 60°. The average kinetic and separation energies of nucleons in these nuclei are deduced. Results of and comments on the radiative correction procedures used in the data analysis are also discussed.

[NUCLEAR REACTIONS ^{6}Li(e,e'), ^{12}C(e,e'), ^{24}Mg(e,e'), ^{40}Ca(e,e'), ^{58,7}Ni(e,e'), ^{89}Y(e,e'), ^{118,7}Sn(e,e'), ^{181}Ta(e,e'), ^{208}Pb(e,e'), $E=500$ MeV, $\theta=60°$; measured $\sigma(E)$; deduced nucleon separation and kinetic energies in Fermi gas model.]

I. INTRODUCTION

In high-energy electron scattering from nuclei the quasielastic peak dominates the spectrum for large-momentum transfer. This peak is believed to be the result of elastic scattering of electrons by individual nucleons in the target nucleus. The elastic electron scattering cross section is always larger for protons than for neutrons and we expect to see this also reflected in quasielastic scattering. Because of the momentum of the nucleons due to their being bound in the nucleus, quasielastic differs from elastic scattering from nucleons in two ways. First, the peak from quasielastic scattering exhibits a Doppler broadening since quasielastic scattering can occur at lower (higher) scattered-electron energy than free electron-nucleon scattering; thus, the motion of the nucleon can decrease (increase) the c.m. energy. Second, the average nucleus-nucleon interaction energy produces a shift of the peak.

Since the interacting nucleon is usually not detected in quasielastic scattering, the direct determination of, for instance, the nucleon-momentum distributions is not available. The interpretation of the quasielastic peak in the scattered-electron spectrum in terms of a "summary" model like the Fermi-gas model[1] is therefore appropriate, provided the model describes the observed spectrum. In such a simplified picture effects like nucleon-nucleon correlations are ignored, even though they could, in principle, produce the effects seen in the observed peak,[2] which increase with decreasing scattered-electron energy. These effects cannot be easily identified because the contributions of processes like π production and N^* excitation can be appreciable and are increasing with excitation energy.

The most obvious information which can be extracted from the quasielastic peak is the average momentum of nucleons in the nucleus, which is related to their Fermi momentum. The Fermi momentum has been previously inferred from the nuclear size, which is a static determination, in contrast to quasielastic scattering which permits a direct dynamic determination. The displacement of the center of the quasielastic peak relative to the free electron-nucleon elastic peak is a measure of the average nucleon separation energies. Such separation energies are of considerable interest since for heavier nuclei only the separation energies of nucleons in the outer shells are known experimentally. Experiments like $(e, e'p)$ or $(p, 2p)$ are designed to measure separation energies, but are plagued with difficulties of interpretation for the heavier nuclei. In addition, proton-induced reactions only have access to outer-shell nucleons.

We have made a series of measurements on the quasielastic peak which span the Periodic Table and from which we extract the nucleon Fermi momentum and nucleon separation energies within the framework of the Fermi gas model of Moniz.[1] Some results from this experiment have been reported previously.[3] Here we present the experimental data, some further discussion of the re-

sults, and detail the problems involved in making the radiative corrections which have previously received little attention.[2,4,5]

II. CORRECTIONS TO THE DATA

The experiment was performed on the Stanford Mark III electron linear accelerator using methods described elsewhere.[3,6] In addition to $(e, e'n)$ and $(e, e'p)$ processes, we expected contributions from $(\gamma, e^{\pm})$, $(\gamma, \pi^{\pm})$, and $(e, e'\pi^{\pm})$ reactions. These backgrounds in the detected electron spectra were determined by reversing the spectrometer magnetic field and measuring the signals resulting from e^+ and π^+ production. These backgrounds, which were never more than 3%, were subtracted from our spectra.

Radiative effects provided a major source of uncertainty in our inelastic electron scattering results. Traditionally, the corrections for radiative effects are applied in two steps. First, the tails from the elastic and narrow prominent inelastic peaks are calculated and then subtracted from the spectra. Second, the inelastic region with its broad peaks is divided into subregions, and each is corrected by integrating over the appropriate interval. However, if the elastic and narrow inelastic peaks are sufficiently small, the first step can be ignored. Such was the case for our data.

Miller derived the equations for radiative corrections to inelastic electron-nucleus scattering, which we summarize in the Appendix.[7] To apply these equations, the inelastic cross sections for scattering over a range of incident energy E and secondary energy E' must be known, the range being determined by the limits on the integrals. Since the radiatively corrected cross section is sought, the integrals must be iterated several times. In an experiment, the cross section is measured at only a few incident energies and an interpolation procedure is used to determine intermediate values. Because the cross sections vary rapidly with energy, data at several intermediate energies must be taken. In this experiment we measured cross sections at $E = 440$, 380, and 320 MeV in addition to the 500-MeV spectra. The scattering angle θ was 60° for all of the spectra.

There are some difficulties attendant to the radiative correction formalism. The function we use is only one form of the peaking approximation to the exact result.[8] The appropriateness of this form for our targets with our kinematics is unknown and requries more theoretical investigation. The correctness of the nuclear bremsstrahlung electron spectrum W could be most easily checked by studying inelastic electron scattering near 0°. This has never been adequately done for any target at any energy. What is usually measured is the photon spectrum from nuclear bremsstrahlung. Miller's formalism is an improvement over previous formulations in that the results are independent to first order of the particular choice of the interval of scattered-electron energy, $\Delta E'$.

We made one experimental check on Miller's radiative correction formalism. Inelastic spectra were measured in the quasielastic region on a naturally abundant iron target, with $E = 500$ MeV, $\theta = 60°$, and target thicknesses of 160 (0.0117), 320 (0.0234), and 640 (0.0467) mg/cm^2 (radiation lengths). Lower incident-energy runs were made on the thinnest target for purposes of radiative corrections. If all three spectra when radiatively corrected are the same, within experimental errors, then our procedure would be correct.

The result was that the corrected spectra were too high on the high-excitation-energy side of the quasielastic peak, the 320 mg/cm^2 target by ~5% and the 640 mg/cm^2 target by ~10%. Because of run time limitations we cannot rule out the possibility that the disagreement may have come from the experimental biases and not only from the radiative correction procedures. Theoretically, the procedures should be valid for targets as thick as 0.1 radiation lengths (rl). For the data presented below we used very thin targets $< 0.01rl$. The target-thickness part of the radiative correction was never more than 20% of the total correction to any data point, which in turn was never more than 30% of the original number of counts.

Because of the fundamental importance of radiative corrections for electron scattering we believe that, in spite of their great difficulty, the calculations to check the accuracy of the peaking approximations and the experiments on zero degree scattering and on targets of varying thickness must be made. For our data the experimental and the radiative correction uncertainties are about equal.

III. RESULTS AND INTERPRETATION

The data from this experiment are listed in Table I and shown in Fig. 1. The radiative corrections have been made as discussed above. The error bars on the data points include uncertainties due to statistics, target-thickness variations, the radiative correction procedure, and background subtractions, but not the ±3% uncertainty due to the proton normalization.[9]

We have compared our data with the Fermi gas model of Moniz[1] where the nuclear Fermi momentum k_F and the average nucleon interaction energy

TABLE I. Proton-normalized and radiative-corrected cross sections $d^2\sigma/d\Omega dE' = (N \pm \Delta N) \times 10^{-n}$ in mb/sr MeV, for $E = 500$ MeV and $\theta = 60°$.

E'	^{6}Li			^{12}C			^{24}Mg			^{40}Ca			$^{58.7}$Ni			^{89}Y			$^{118.7}$Sn			$^{180.95}$Ta			^{208}Pb		
(MeV)	N	ΔN	n	N	ΔN	n	N	ΔN	n	N	ΔN	n	N	ΔN	n	N	ΔN	n	N	ΔN	n	N	ΔN	n	N	ΔN	n
480.0	···			1.79	0.19	7	3.83	0.42	7	···			1.22	0.17	6	1.71	0.19	6	···			···			···		
474.0	···			1.02	0.13	7	···			···			···			···			···			···			···		
470.0	1.72	0.18	7	5.75	0.52	7	1.55	0.15	6	···			3.90	0.29	6	5.85	0.41	6	···			7.09	0.67	6	7.00	0.68	6
464.0	2.49	0.29	7	1.38	0.11	6	1.91	0.17	6	2.72	0.15	6	4.48	0.33	6	5.68	0.37	6	8.32	0.71	6	1.16	0.08	5	9.82	0.79	6
460.0	2.96	0.30	7	1.20	0.09	6	2.58	0.19	6	···			···			···			···			1.54	0.10	5	1.81	0.10	5
454.1	5.02	0.47	7	9.21	0.71	7	2.96	0.20	6	4.20	0.17	6	7.00	0.41	6	1.07	0.05	5	1.85	0.09	5	1.70	0.11	5	2.31	0.11	5
450.0	···			···			···			···			8.92	0.47	6	1.03	0.05	5	1.83	0.09	5	···			···		
444.3	8.68	0.58	7	1.26	0.07	6	4.11	0.25	6	6.67	0.27	6	1.02	0.05	5	1.33	0.05	5	···			2.77	0.14	5	2.74	0.12	5
440.0	1.11	0.06	6	2.59	0.13	6	5.23	0.26	6	···			···			···			···			3.43	0.16	5	3.24	0.13	5
434.2	1.32	0.06	6	2.99	0.14	6	5.50	0.26	6	8.74	0.35	6	1.19	0.05	5	1.90	0.07	5	2.27	0.09	5	3.14	0.15	5	3.34	0.14	5
430.0	···			···			···			···			1.40	0.07	5	2.11	0.08	5	2.77	0.11	5	···			···		
424.3	2.12	0.08	6	3.75	0.15	6	7.31	0.29	6	1.12	0.04	5	1.54	0.08	5	2.31	0.09	5	2.88	0.12	5	4.43	0.18	5	4.74	0.19	5
414.4	2.88	0.12	6	4.75	0.19	6	8.78	0.35	6	1.32	0.05	5	1.78	0.10	5	2.88	0.11	5	3.40	0.14	5	4.98	0.20	5	5.64	0.23	5
404.5	3.51	0.14	6	5.46	0.22	6	1.02	0.04	5	1.56	0.06	5	2.09	0.08	5	3.09	0.12	5	3.90	0.16	5	5.89	0.24	5	6.57	0.26	5
400.0	···			6.25	0.25	6	1.09	0.04	5	···			2.35	0.09	5	3.34	0.13	5	4.29	0.17	5	6.56	0.27	5	7.00	0.28	5
394.7	4.16	0.17	6	6.32	0.26	6	1.15	0.05	5	1.75	0.07	5	2.22	0.09	5	3.41	0.14	5	4.56	0.18	5	6.29	0.25	5	7.25	0.29	5
385.7	4.55	0.18	6	7.09	0.28	6	1.21	0.05	5	1.86	0.07	5	2.51	0.10	5	3.91	0.16	5	4.88	0.19	5	6.36	0.26	5	7.88	0.32	5
374.9	4.76	0.19	6	6.97	0.28	6	1.33	0.05	5	1.94	0.08	5	2.72	0.11	5	4.02	0.16	5	4.88	0.19	5	6.87	0.28	5	8.19	0.33	5
365.0	4.56	0.18	6	7.28	0.29	6	1.32	0.05	5	2.08	0.08	5	2.69	0.10	5	4.04	0.16	5	5.34	0.21	5	7.77	0.31	5	8.61	0.34	5
360.0	4.50	0.18	6	6.61	0.28	6	1.32	0.05	5	···			2.88	0.11	5	4.11	0.16	5	5.69	0.23	5	7.92	0.33	5	8.42	0.34	5
355.2	4.35	0.17	6	6.97	0.28	6	1.36	0.05	5	2.08	0.08	5	2.69	0.11	5	4.23	0.17	5	5.22	0.21	5	7.51	0.30	5	···		
345.3	3.68	0.15	6	6.54	0.26	6	1.35	0.05	5	1.85	0.07	5	2.72	0.11	5	4.02	0.16	5	5.37	0.21	5	7.59	0.30	5	8.83	0.35	5
335.4	2.90	0.12	6	5.91	0.24	6	1.29	0.05	5	1.87	0.08	5	2.48	0.10	5	4.08	0.16	5	4.92	0.19	5	7.44	0.29	5	8.68	0.35	5
325.5	2.59	0.10	6	5.23	0.21	6	1.05	0.04	5	1.61	0.07	5	2.48	0.11	5	3.78	0.15	5	4.83	0.19	5	6.93	0.28	5	7.81	0.31	5
320.0	···			···			···			···			2.35	0.09	5	3.34	0.14	5	4.53	0.18	5	···			···		
315.7	2.16	0.10	6	4.43	0.18	6	9.41	0.38	6	1.47	0.06	5	2.26	0.09	5	3.43	0.14	5	4.34	0.17	5	6.61	0.26	5	7.76	0.31	5
305.8	1.84	0.09	6	3.79	0.15	6	8.61	0.32	6	1.23	0.05	5	2.03	0.08	5	3.27	0.13	5	4.32	0.17	5	6.11	0.24	5	6.92	0.28	5
300.0	···			···			···			···			1.97	0.08	5	3.11	0.12	5	4.03	0.16	5	···			···		
295.9	1.55	0.09	6	3.38	0.14	6	6.77	0.29	6	9.97	0.40	6	1.80	0.07	5	3.02	0.12	5	3.74	0.15	5	5.38	0.22	5	6.73	0.27	5
285.9	1.50	0.09	6	2.96	0.14	6	6.64	0.31	6	9.73	0.39	6	1.72	0.07	5	2.60	0.13	5	3.55	0.15	5	4.92	0.23	5	6.30	0.29	5
276.2	1.14	0.08	6	2.64	0.13	6	6.03	0.32	6	8.35	0.41	6	1.50	0.07	5	2.64	0.13	5	3.10	0.15	5	5.22	0.24	5	5.73	0.30	5
266.3	1.08	0.08	6	2.61	0.14	6	5.32	0.33	6	8.57	0.43	6	1.31	0.08	5	2.37	0.14	5	2.72	0.16	5	4.62	0.26	5	5.51	0.31	5
260.0	···			···			···			···			1.39	0.08	5	1.95	0.13	5	2.94	0.18	5	···			···		
256.4	1.28	0.09	6	2.43	0.15	6	5.71	0.35	6	8.33	0.45	6	1.27	0.08	5	2.27	0.14	5	2.87	0.18	5	4.57	0.28	5	5.63	0.33	5
246.6	1.20	0.09	6	2.55	0.16	6	5.47	0.36	6	8.55	0.48	6	1.39	0.09	5	2.14	0.14	5	2.95	0.19	5	4.33	0.28	5	5.40	0.35	5
236.7	1.15	0.10	6	2.54	0.16	6	5.18	0.38	6	8.71	0.51	6	1.34	0.09	5	2.24	0.15	5	3.02	0.20	5	4.35	0.30	5	4.90	0.34	5
226.8	1.27	0.11	6	2.88	0.19	6	5.62	0.42	6	8.72	0.51	6	1.29	0.10	5	2.29	0.16	5	2.73	0.20	5	4.57	0.30	5	5.88	0.37	5
216.9	1.43	0.14	6	2.94	0.21	6	6.35	0.49	6	9.81	0.56	6	1.34	0.10	5	2.38	0.17	5	3.26	0.22	5	5.42	0.36	5	5.76	0.38	5
207.0	1.66	0.16	6	2.94	0.21	6	6.59	0.52	6	1.02	0.06	5	1.43	0.11	5	2.51	0.18	5	3.24	0.22	5	5.58	0.37	5	6.11	0.40	5
197.2	1.78	0.17	6	3.42	0.24	6	7.01	0.59	6	···			1.59	0.12	5	2.77	0.20	5	3.43	0.24	5	5.67	0.38	5	5.99	0.41	5

$\bar{\epsilon}$ are variable parameters. The quasielastic peak width is directly proportional to k_F and the peak location determines $\bar{\epsilon}$. Since for the kinematics of the present experiment the electron-proton scattering cross section is about seven times larger than the one for neutrons, k_F and $\bar{\epsilon}$ essentially refer to the protons.[3]

Since the data extend well beyond the pion threshold, an estimate of the pion electroproduction cross section is included in the calculations. This is also computed in the Fermi gas model and has been taken as the sum of two contributions. First, s-wave production is calculated following the method of Czyż and Walecka,[10] the only improvement being that the pion is assumed not to be close to threshold in the integration-over-pion coordinates. Second, pion production proceeding through excitation of the first nucleon resonance is computed using the isobar model of Moniz with a realistic line shape for the 3-3 resonance folded in.[11] The interference term between s-wave and resonance production has been neglected and coherent π^0 production has been found to be negligible even for lead.

Moniz's model gives a good fit to the quasielastic data as is shown in Fig. 1. In particular, it should be noted that the absolute value of the cross section is well reproduced, even for the heaviest nuclei. Since we observe only the scattered electron, we have no problems with the strong absorption of the quasielastically scattered nucleon on its way out of the nucleus.

The fitted values of $\bar{\epsilon}$ and k_F are given in Ref. 3. However, for ^{40}Ca, $\bar{\epsilon}$ is 5 MeV lower than our previous results. Reference 11 shows that, if the relativistic recoil of the nucleon is included, the values of k_F and $\bar{\epsilon}$ increase by approximately 5 MeV/c from our results.[10] The roughly constant value of k_F at ~260 MeV/c from nickel through lead is expected from the saturation of nuclear forces. The inferred saturated nuclear matter density from elastic electron scattering of ρ

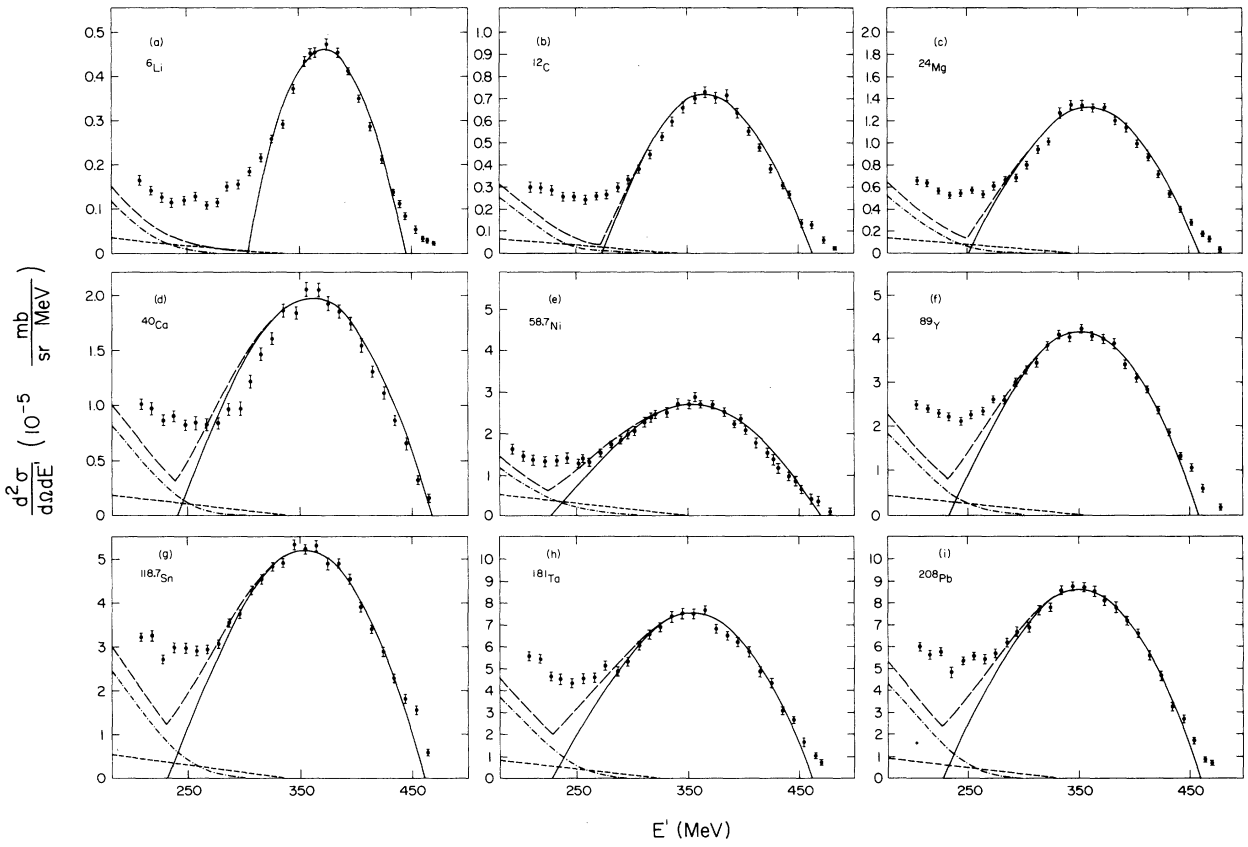

FIG. 1. The measured quasielastic peaks; the errors on the data points do not include an over-all 3% normalization uncertainty. The solid curve is a fit by the Fermi-gas model which yielded k_F (in MeV/c) and $\bar{\epsilon}$ (in MeV) as follows: (a) ^{6}Li (169, 17); (b) ^{12}C (221, 25); (c) ^{24}Mg (235, 32); (d) ^{40}Ca (249, 33); (e) $^{58.7}$Ni (260, 36); (f) ^{89}Y (254, 39); (g) $^{118.7}$Sm (260, 42); (h) ^{181}Ta (265, 42); (i) ^{208}Pb (265, 44). The fitting uncertainty in k_F is ±5 MeV/c and in $\bar{\epsilon}$ it is ±3 MeV. The small-amplitude dashed curve is the s-wave π-production contribution, the dot-dashed curve is the isobar excitation, and the large-amplitude dashed curve is the total result.

$\approx 0.17 f_m^{-3}$ gives an equivalent Fermi momentum $k_F = (3\pi^2\rho/2)^{1/3} \simeq 270$ MeV/c. The small difference can be attributed to surface effects. For the lighter nuclei, where a comparison with the $\bar{\epsilon}$ obtained from $(e, e'p)$ and $(p, 2p)$ can be made, we find, within the quoted uncertainties, the same average separation energy. For the heavier nuclei our value of $\bar{\epsilon}$ is surprisingly large.

Although the absolute cross section is fitted well by the Fermi gas model, there is a systematic underestimation of the observed cross section at very large energy loss which is not understood. This cannot be attributed to the N^* production because Moniz's model has also been observed to work well in the N^* region.[12-14] A model which includes effects of final-state interactions, nucleon-nucleon short-range correlations, a more complicated momentum distribution, and the nuclear surface might explain the excess cross section. More detailed experimental results such as measurements of the longitudinal and transverse parts as a function of momentum transfer or $(e, e'p)$ coincidence experiments would be desirable. Nevertheless the Fermi gas model with just k_F and $\bar{\epsilon}$ as parameters reproduces the systematics and the general behavior of the quasielastic region surprisingly well.

IV. ACKNOWLEDGMENTS

The authors wish to thank Professor Ernest J. Moniz for his assistance in applying his calculations to these data, and Professor Robert Hofstadter and Professor Mason R. Yearian and the staff of the High Energy Physics Laboratory for their support.

APPENDIX

The doubly differential cross section in terms of the solid angle Ω and scattered electron energy E' can be written for incident electron energy E as:

$$\frac{d\sigma}{d\Omega dE'}(E, E', \theta) = \left[\left(\frac{\Delta E}{E}\right)^{t/2+bt_b}\left(\frac{\Delta E'}{E'}\right)^{t/2+bt_a}\left(\frac{1+\delta'(q^2)}{\Gamma(1+bt_b+bt_a)}\right)\right]^{-1}$$

$$\times\left[\frac{d\sigma_R(E, E', \theta)}{d\Omega dE'} + \frac{d\sigma_{ER}(E, E', \theta)}{d\Omega dE'}\right.$$

$$-\int_{E_{\min}}^{E-\Delta E} dE_1\left(\frac{v_b}{E-E_1} + t_b W(E, E_1)\right)\frac{d\sigma(E_1, E', \theta)}{d\Omega dE'}\left(\frac{k_1}{E}\right)^{t/2+bt_b}\left(\frac{k_1'}{E'}\right)^{t/2+bt_a}\left(\frac{1+\delta'(q_1^2)}{\Gamma(1+bt_b+bt_a)}\right)$$

$$\left.-\int_{E'+\Delta E'}^{E'_{\max}} dE_1'\left(\frac{v_a}{E_1'-E'} + t_a W(E_1', E')\right)\frac{d\sigma(E, E_1', \theta)}{d\Omega dE'}\left(\frac{k_1}{E}\right)^{t/2+bt_b}\left(\frac{k_1'}{E'}\right)^{t/2+bt_a}\left(\frac{1+\delta'(q_1^2)}{\Gamma(1+bt_b+bt_a)}\right)\right]$$

where $\hbar = c = 1$ and $d\sigma_R/d\Omega dE'$ and $d\sigma_{ER}/d\Omega dE'$ are the radiated and elastic radiated cross sections, respectively. α is the fine structure constant, m the mass of the electron, N the number of target atoms/cm^3, Z the nuclear charge, and r_0 the classical electron radius. Defining two functions

$$D = \ln(191\ Z^{-3}) - 1.2(\alpha Z)^2,$$

$$\zeta = \ln(1440\ Z^{-2/3}),$$

the radiation length in g/cm^2 is

$$X_0 = [4N\alpha r_0^2 DZ(Z+\zeta)]^{-1},$$

$$a = \left(\frac{1}{9D}\right)\left(\frac{Z+1}{Z+\zeta}\right),$$

and

$$b = a + \tfrac{4}{3}.$$

The half-target-plus-exit(entrance)-window thickness is $t_a(t_b)$ in radiation lengths and

$$W(E, E') = \frac{1}{E-E'}\left[1 + \left(\frac{E'}{E}\right)^2 - \frac{E'}{E}\left(\tfrac{2}{3} - a\right)\right].$$

The scattering angle of the electron, θ, the mass of the target nucleus, M, and the four-momentum transfer to the electron, $q^2 = 4EE'\sin^2\tfrac{1}{2}\theta$, can be combined to define

$$\delta'(q^2) = (2\alpha/\pi)\left[\tfrac{13}{12}\ln(q^2/m^2) - \tfrac{14}{9}\right],$$

$$t = (2\alpha/\pi)[\ln(q^2/m^2) - 1],$$

$$v_b = \tfrac{1}{2}t[E'/E + \tfrac{3}{4}(1 - E'/E)^2],$$

and

$$v_a = \tfrac{1}{2}t[E'/E_1' + \tfrac{3}{4}(1 - E'/E)^2].$$

The remaining kinetic terms in the integrals are

defined in the following manner:

$$\eta = 1 + \frac{2E}{M}\sin^2(\tfrac{1}{2}\theta), \qquad \eta' = \left[1 - \frac{2E'}{M}\sin^2(\tfrac{1}{2}\theta)\right]^{-1},$$

$$w = E - \eta' E', \qquad w' = E/\eta - E',$$

$$q_1^2 = 4E_1 E' \sin^2(\tfrac{1}{2}\theta), \qquad q_1'^2 = 4EE_1' \sin^2(\tfrac{1}{2}\theta),$$

$$k_1 = \min(E/3, w_1), \qquad k_1' = \min(E'/3, w_1'),$$

where $w_1 = E - E_1$ and $w_1' = w'/\eta\eta'$ for E integral, and where $w_1' = E_1' - E'$ and $w_1 = \eta\eta' w'$ for E' integral. The limits of the integrals are defined as:

$$E_{\min} = E'/\eta', \quad E'_{\max} = E/\eta, \text{ and } \Delta E = \eta\eta'\Delta E',$$

where $\Delta E' = E' - E'_{\min}$.

The above result does not include effects of ionization loss and broadening, which are of significant size at low energies. The ionization loss can, however, be accounted for by adjusting the incident and/or scattered electron energies by this loss.

---

*Present address: Department of Physics, University of Massachusetts, Amherst, Massachusetts 01002.

†Present address: Department of Physics, University of Basel, Basel, Switzerland. Work supported in part by the Swiss National Science Foundation.

‡Work supported in part by the National Science Foundation and Office of Naval Research under Contract No. Nonr 225(67).

§Present address: Department of Physics, State University of New York, Stony Brook, New York 11790.

¶Work supported in part by a grant from the Petroleum Research Fund of the American Chemical Society.

[1]E. J. Moniz, Phys. Rev. 184, 1154 (1969).

[2]W. Czyż and K. Gottfried, Ann. Phys. (N. Y.) 21, 47 (1963).

[3]E. J. Moniz, I. Sick, R. R. Whitney, J. R. Ficenec, R. D. Kephart, and W. P. Trower, Phys. Rev. Lett. 26, 445 (1971).

[4]P. Zimmerman, Ph.D. thesis, Stanford University, 1969 (unpublished).

[5]D. B. Isabelle and J. Berthot, presented at NATO Institution on Electron Scattering and Nuclear Structure, Cagleori, 1970 (to be published).

[6]I. Sick and J. S. McCarthy, Nucl. Phys. A150, 631 (1970).

[7]G. Miller, Ph.D. thesis, Stanford University, 1970 (unpublished); and Stanford Linear Accelerator Center Report No. 129, 1971.

[8]L. W. Mo and Y. S. Tsai, Rev. Mod. Phys. 41, 205 (1969).

[9]T. Janssens, R. Hofstadter, E. B. Hughes, and M. R. Yearian, Phys. Rev. 142, 922 (1966).

[10]W. Czyż and J. P. Walecka, Nucl. Phys. 51, 312 (1964).

[11]R. A. Smith and E. J. Moniz, Nucl. Phys. B43, 605 (1972).

[12]Yu. I. Titov, E. V. Stepula, N. G. Afanos'ev, R. V. Akhmerov, S. A. Byvalin, N. F. Severin, and E. M. Smelov, Yad. Fiz. 13, 1149 (1971) [transl.: Sov. J. Nucl. Phys. 13, 660 (1971)].

[13]The apparent disagreement between experiment and theory shown in Ref. 12 comes from a minus sign misprint in Appendix A of the original paper of Moniz. An analysis can be found in E. J. Moniz, Los Alamos Meson Physics Facility Internal Report, 1972 (unpublished), showing the agreement between the quasielastic experimental and theoretical results.

[14]K. C. Stanfield, C. R. Canizares, W. L. Faissler, and F. M. Pipkin, Phys. Rev. C 3, 1448 (1971).